Solution and Solid-State Studies of Alkali Metal Aggregate Assemblies

John Jacob Morris

Publication Date

07-04-2008

CHAPTER 3

SYSTEMATIC STUDY OF REACTION ADDITIVES ON THE MOLECULAR AND NETWORK STRUCTURE OF LITHIUM 2,4,6-TRISUBSTITUTED ARYLOXIDE COMPLEXES

3.1 Introduction

Our group has previously shown that molecular cage aggregates of *s*-block metal complexes can successfully be utilized as secondary building units (SBUs) to direct network assembly.[1] For example, tetrameric cubanes of specific lithium aryloxides, $(ArOLi)_4$, may be designed such that each metal center has a single open site for coordination to a Lewis base.[1a] In turn, employment of a ditopic linker results in these aggregates acting as tetrahedral nodes to form diamondoid networks (Figure 3.1a). Similarly, Na_6O_6 hexameric aggregates may be employed as octahedral nodes to construct cubic frameworks (Figure 3.1b).[1b] We were interested in expanding the scope of our work to alternative types of well-characterized *s*-block aggregates and targeted the preparation of tetrasolvated dimeric complexes of lithium aryloxides, $[(ArOLi{\cdot}D_2)_2]$, where D = monodentate Lewis base. These are appealing SBU candidates since they are readily accessible by suitable tuning of both the electronics and substitution pattern of the aryloxide ligand.[2] They are also smaller and lighter than the tetrameric cubanes, which is of interest to material chemists interested in the preparation of low molecular weight

materials for the storage of small molecules such as dihydrogen.[3] The tetrasolvated dimers also differ from the previously employed aggregates as they possess two, rather than one, well-defined potential points of extension from each metal *i.e.* two donor solvents per lithium (Figure 3.1c). We reasoned that if all four coordination sites could be linked to neighboring aggregates the dimeric SBUs would act as tetrahedral nodes and, in turn, build 3D diamondoid networks.[4] A reasonable alternative is that the dimers could act as square planar nodes if the pairs of bridging ligands on each metal center extend along the same plane.

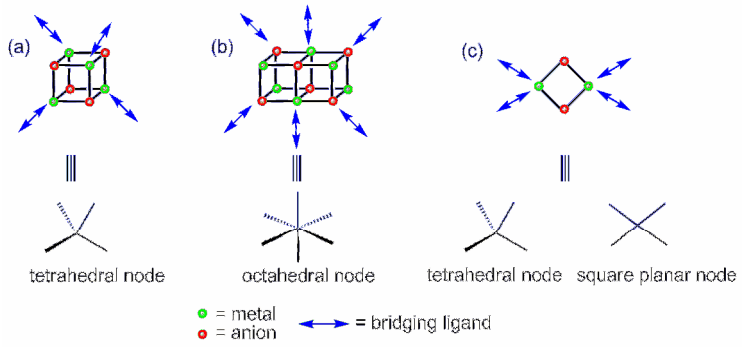

Figure 3.1 Relationship between selected metal aggregates and their potential nodal geometries: (a) tetrasolvated tetrameric cubane, (b) hexasolvated prismatic hexamer, (c) tetrasolvated ring dimer.

Several coordination polymers composed of lithiated ring dimers have previously been characterized, although these have usually been prepared inadvertently rather than by design.[5,6] These polymers fall into two main categories: 1D polymeric chains[5] and 2D square (4,4) sheets.[6] Simple 1D chains are most commonly produced via bridging of the dimers by a didentate base, as seen for $[\{(^{t}BuCH_2)PhNLi\}_2\cdot(tmeda)]_\infty$.[5a] The dimers can therefore be considered to be linear nodes in these species. The 2D square nets normally employ anions that contain a non-chelating Lewis base which links between neighboring dimers, as exemplified by $[(RO)_2P(O)CHC{\equiv}NLi\cdot(thf)]_\infty$, where R = Et or ^{i}Pr.[6a] In these

instances the dimers can be considered to be square-planar nodes. There are no examples of Li_2X_2 ring dimers, where X = any atom, acting as tetrahedral nodes to give 3D networks.

The second goal of this project was to control network formation using reaction additives. This would serve as a complement to the work described in the previous chapter using heteroleptic aggregates to control the network topology. By adding a strong monodentate donor to our lithium aryloxide dioxane reaction mixtures, we hoped to influence the dimensionality of the resulting network by blocking available metal sites. More specifically, we were interested in the stepwise replacement of divergent dioxane with terminal dimethylformamide (DMF) in the lithium aryloxide system.

3.2 Reactions of Lithium 4-Cl-2,6-Dimethylphenoxide

3.2.1 Synthesis

The equimolar reaction of 4-Cl-2,6-dimethylphenol with BuLi in 1,4-dioxane resulted in the instant formation of a precipitate, which dissolved on vigorous heating. High-quality crystals of $[(4\text{-Cl-2,6-Me}_2\text{-C}_6\text{H}_2\text{OLi})_2\cdot(\text{dioxane})_2]_\infty$ (**3.1**) were grown from the reaction solution after optimizing the concentration and temperature for crystal growth. Subsequent equimolar reactions of 4-Cl-2,6-dimethylphenol with BuLi in 1,4-dioxane with varying amounts of DMF or toluene resulted in the formation of $[(4\text{-Cl-2,6-Me}_2\text{-C}_6\text{H}_2\text{OLi})_2\cdot(\text{dioxane})_{2.5}]_\infty$ (**3.2**), $[(4\text{-Cl-2,6-Me}_2\text{-C}_6\text{H}_2\text{OLi})_4\cdot(\text{dmf})_4]$ (**3.3**), $[(4\text{-Cl-2,6-Me}_2\text{-C}_6\text{H}_2\text{OLi})_4\cdot(\text{dioxane})\cdot(\text{dmf})_2]_\infty$ (**3.4**), or $[(4\text{-Cl-2,6-Me}_2\text{-C}_6\text{H}_2\text{OLi})_4\cdot(\text{dioxane})_2]_\infty$ (**3.5**) depending on the reaction conditions. Finally, the equimolar reaction of 4-Cl-2,6-

dimethylphenol with BuLi in 1,3-dioxolane resulted in the formation of $[(4\text{-Cl-2,6-Me}_2\text{-C}_6\text{H}_2\text{OLi})_2\cdot(\text{dioxolane})_2]_\infty$ (**3.6**).

3.2.2 Solid-State Structures

For our initial study, we targeted the lithium 4-Cl-2,6-dimethylphenoxide dioxane system. The archetypal compound, $[(4\text{-Cl-2,6-Me}_2\text{-C}_6\text{H}_2\text{OLi})_2\cdot(\text{dioxane})_2]_\infty$ (**3.1**), is a dimer composed of two lithium atoms and two μ_2-aryloxides (Figure 3.2a). Both of the lithium atoms are coordinated by two ditopic dioxane molecules. The Li-O_{Ar} bond distances are noticeably shorter than the Li-O_{Ar} bond distances seen in the tetrameric and hexameric aggregates detailed in the previous chapter. A selection of important metrical parameters is highlighted in Table 3.1. The mean Li-O_{Ar} distance in **3.1** is 1.861 Å (range of 1.850(1) – 1.866(1) Å), whereas the mean Li-O_{Ar} distance in the tetrameric aggregate **2.1** is 1.997(5) Å (range of 1.959(5)-2.045(5) Å). This shortening can be attributed to the lithium centers in **3.1** bonding to μ_2-aryloxides as opposed to μ_3-aryloxides in **2.1**. The mean Li-O_{diox} distance in **3.1** of 2.014 Å (range of 1.989(2) – 2.054(2) Å) is only slightly longer than in **2.1** of 1.992 Å (range of 1.937(5)-2.049(5) Å). This slight increase can be attributed to a number of factors including the change in aggregation state, the electron-withdrawing chloride group at the *para*-position of the aryloxide, or crystal packing effects. Since the lithium dimer acts as a square planar node the resulting extended structure is a two-dimensional 4^4-net (Figure 3.2c).

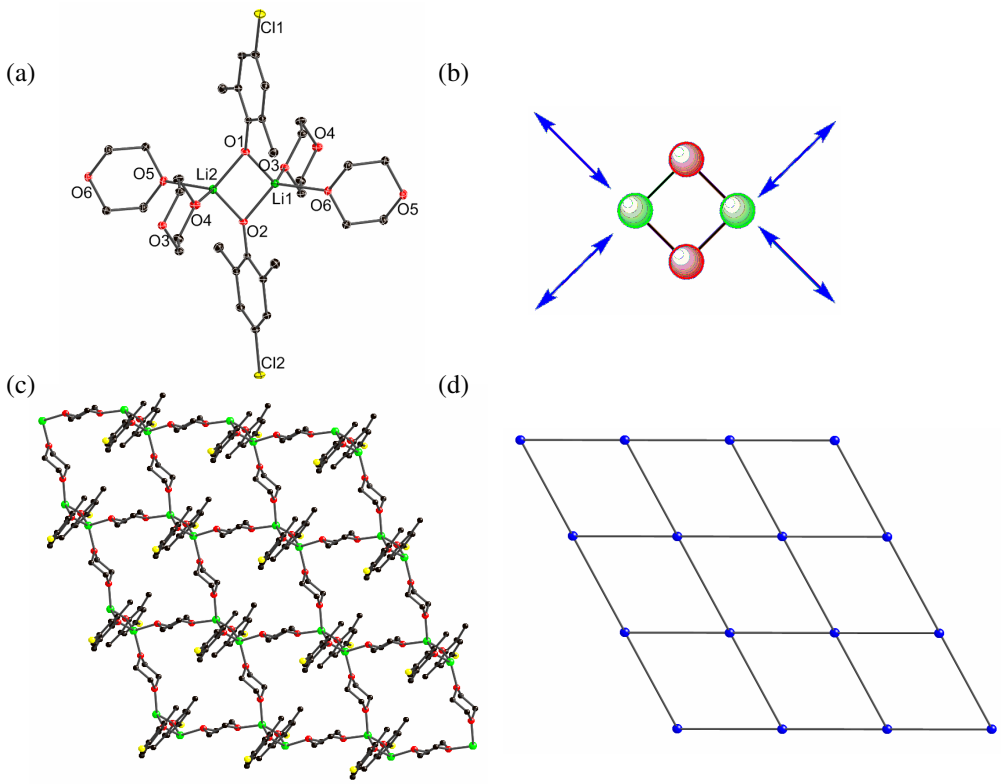

Figure 3.2 (a) The tetrasolvated dimeric aggregate of **3.1** with two dioxane molecules solvating each lithium center. (b) Illustration of the dimeric aggregate as a square planar node with bridging dioxane shown as blue arrows. (c) The extended two-dimensional network of **3.1** with a 4^4-net topology. (d) Simplification of the 4^4-network with the dimeric aggregates shown as blue spheres and the dioxanes as the gray connections.

Since there are four divergent dioxane molecules coordinated to each dimer, our goal going forward on this project was the stepwise replacement of each dioxane molecule with a terminal DMF. As shown in Scheme 3.1 our expectation was that the following reduction in network structure would occur: (i) a 2D 4^4-net with no DMF present, (ii) a 2D 6^3-net with 1 eq. of DMF per dimer present, (iii) a 1D polymer with 2 eq. DMF present, (iv) a 0D dumbbell with 3 eq. DMF present, and (v) a molecular DMF solvate with 4 eq. DMF present. The following structures summarizes our work towards this goal of network reduction.

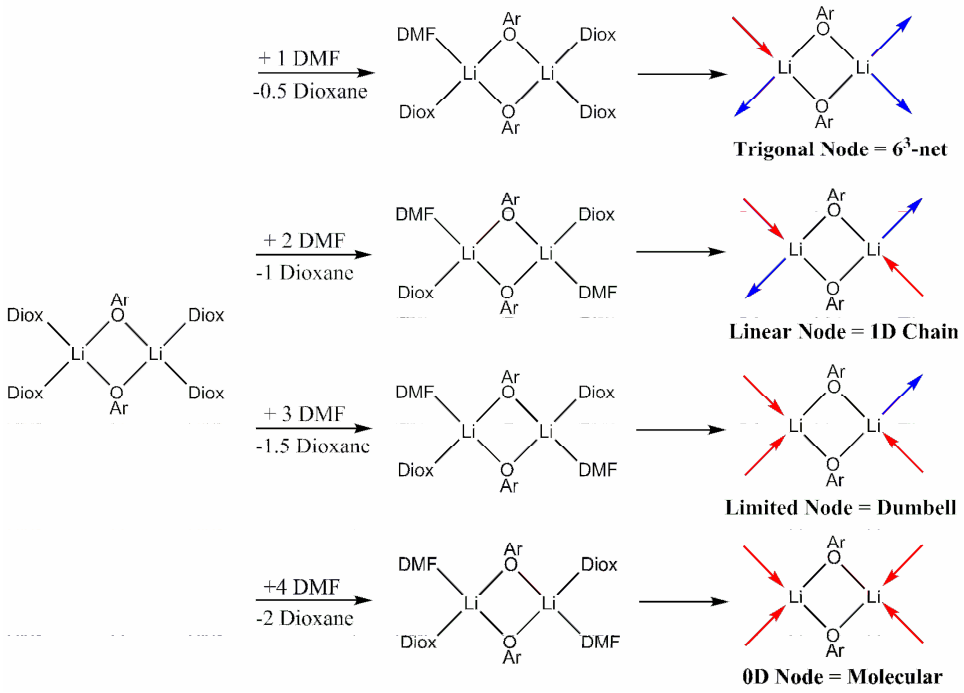

Scheme 3.1 Proposed sequential replacement of dioxane by DMF starting with the tetrasolvated dimeric aggregate **3.1**. The amount of each Lewis base is relative to the dimer. The dioxane is half the amount of DMF in each step because it is a divergent solvate that bridges between aggregates.

By adding 0.5 equivalents of DMF per lithium (or 1 eq. of DMF per dimer), we predicted that one of the four dioxane coordination sites on the dimer would be replaced by terminal DMF. This would allow the dimer to have only three points of extension, which should give a hexagonal 6^3-net. The synthesized compound, $[(4\text{-Cl-}2,6\text{-Me}_2\text{-}C_6H_2OLi)_2\cdot(\text{dioxane})_{2.5}]_\infty$ (**3.2**), forms a dimer composed of two lithium atoms and two μ_2-aryloxides (Figure 3.3a). The metrical parameters of the dimer remains relatively unchanged compared to **3.1**, with a mean Li-O_{Ar} bond distance of 1.896 Å. The dimer is coordinated by three bridging dioxane molecules, but instead of the expected terminal DMF on the fourth lithium site, there is a terminal dioxane. However, the dimeric aggregate does act as the targeted trigonal node with three dioxanes bridging to other aggregates to give a two-dimensional 6^3-net (Figure 3.3c). The homogeneity of the bulk

crystalline product for both **3.1** and **3.2** was checked by a combination of multiple unit cell checks on each sample, powder diffraction of the bulk products, and ^{1}H NMR analysis.

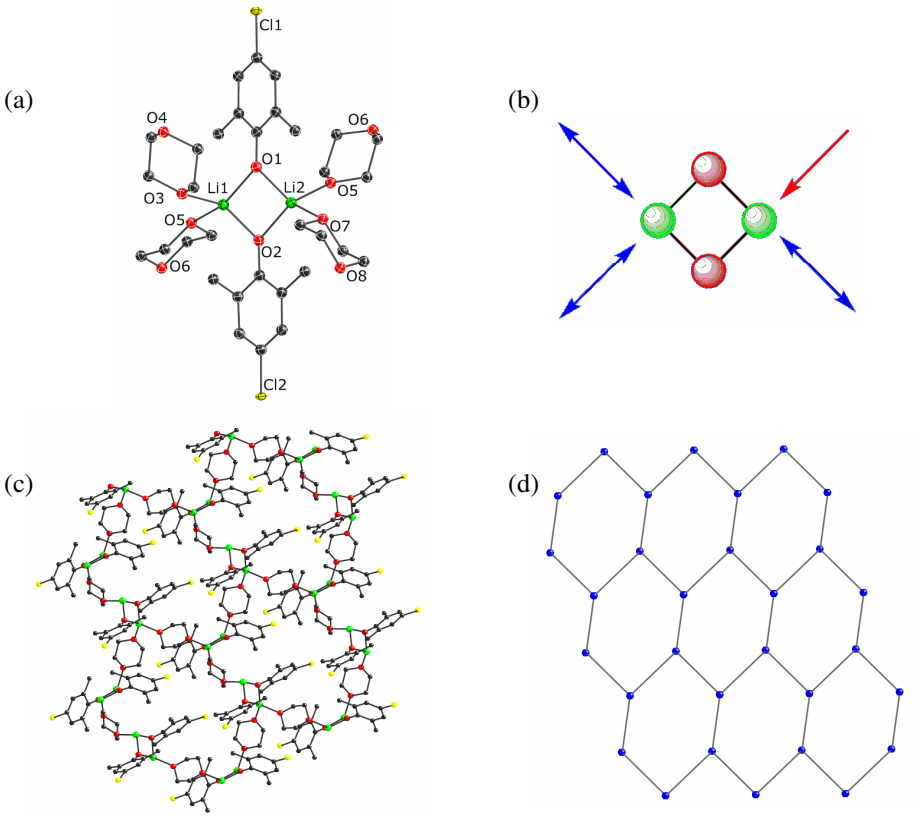

Figure 3.3 (a) Tetrasolvated dimeric aggregate of **3.2** with two dioxane molecules solvating each lithium center (b) Illustration of the dimeric aggregate as a trigonal node with the three bridging dioxane shown as blue arrows and the one terminal dioxane shown as a red arrow. (c) The extended two-dimensional network of **3.2** with 6^3-net topology. The terminal dioxane molecule on each dimer has been removed for clarity. (d) Simplification of the 6^3-network with the dimeric aggregates shown as blue spheres and the bridging dioxane as the gray connections.

TABLE 3.1

KEY BONDS LENGTHS [Å] AND ANGLES (°) FOR **3.1**-**3.10.** MEAN PARAMETERS ARE IN BRACKETS

	M-O_{Ar}	**M-$O_{Dioxane}$**	**M-O_{DMF}**	**O_{Ar}-M-O_{Ar}**	**M-O_{Ar}-M**
3.1	1.850(1) – 1.866(1) <1.861>	1.989(2) – 2.054(2) <2.014>	—	95.38(7), 95.79(7)	84.19(6), 84.53(6)
3.2	1.871(4) – 1.937(4) <1.896>	1.983(4) – 2.078(4) <2.024>	—	93.57(19) – 96.60(17) <94.71>	83.67(16) – 86.35(18) <85.26>
3.3	1.978(3) – 2.030(3) <2.001>	—	1.937(3)	94.33(11) – 95.97(11) <95.05>	83.94(10) – 85.31(11) <84.71>
3.4	1.922(2) – 2.049(2) <1.989>	2.125(2)	1.922(2)	92.47(6) – 98.15(6) <94.83>	82.13(6) – 86.30(6) <84.87>
3.5	1.894(3) – 2.090(3) <1.966>	1.982(3) – 2.131(3) <2.042>	—	89.75(13) – 100.51(14) <95.10>	81.18(13) – 89.96(13) <84.58>
3.6	1.871(3) – 1.906(3) <1.890>	2.041(3) – 2.085(3)[a] <2.061>	—	91.69(14) – 93.9(2) <92.56>	87.02(14), 88.25(14)
3.7	1.874(3) – 1.933(3) <1.894>	1.996(3) – 2.066(13) <2.017>	—	94.22(14) – 95.72(15) <94.96>	83.75(14) – 85.60(14) <85.01>
3.8	1.919(2) – 2.062(2) <1.995>	2.159(2)	1.928(2)	92.17(9) – 98.14(10) <94.70>	81.92(9) – 87.00(9) <85.00>
3.9	1.970(2) – 2.029(2) <1.998>	—	1.941(2)	94.23(9) – 95.92(9) <95.00>	84.00(9) – 85.41(9) <84.76>
3.10	1.875(4) – 1.920(4) <1.898>	2.052(3) – 2.082(4)[a] <2.070>	—	90.9(2) – 93.8(2) <92.0>	87.4 (2), 89.2(2)

[a] Values reported for the M-$O_{Dioxolane}$ bond distance

Thus, the addition of DMF clearly affects the resulting solid-state structure but not in the manner anticipated. To investigate this unexpected behavior further a ^{1}H NMR titration study was conducted. Lithium 4-Cl-2,6-dimethylphenoxide was dissolved in dioxane with a d_{12}-cyclohexane spike. Measured amounts of DMF were then titrated into the solution and the ^{1}H NMR spectra collected. It was expected that coordinated DMF would have a significant upfield shift of both the formyl and methyl protons in the spectra compared with free DMF in neat dioxane (Figure 3.4a). Upon the first addition of DMF (0.l25 eq. per lithium) the upfield shift is indeed seen (Figure 3.4b). This suggests that DMF is coordinating to the lithium dimer. The addition of more DMF to the NMR solution (0.25 – 2.00 eq. per lithium) shows a continual downfield shift of the protons in the ^{1}H NMR spectra. This suggests that DMF coordination is still occurring, but there is a dynamic equilibrium between free and coordinated DMF on the NMR time scale (Figure 3.4c-f).

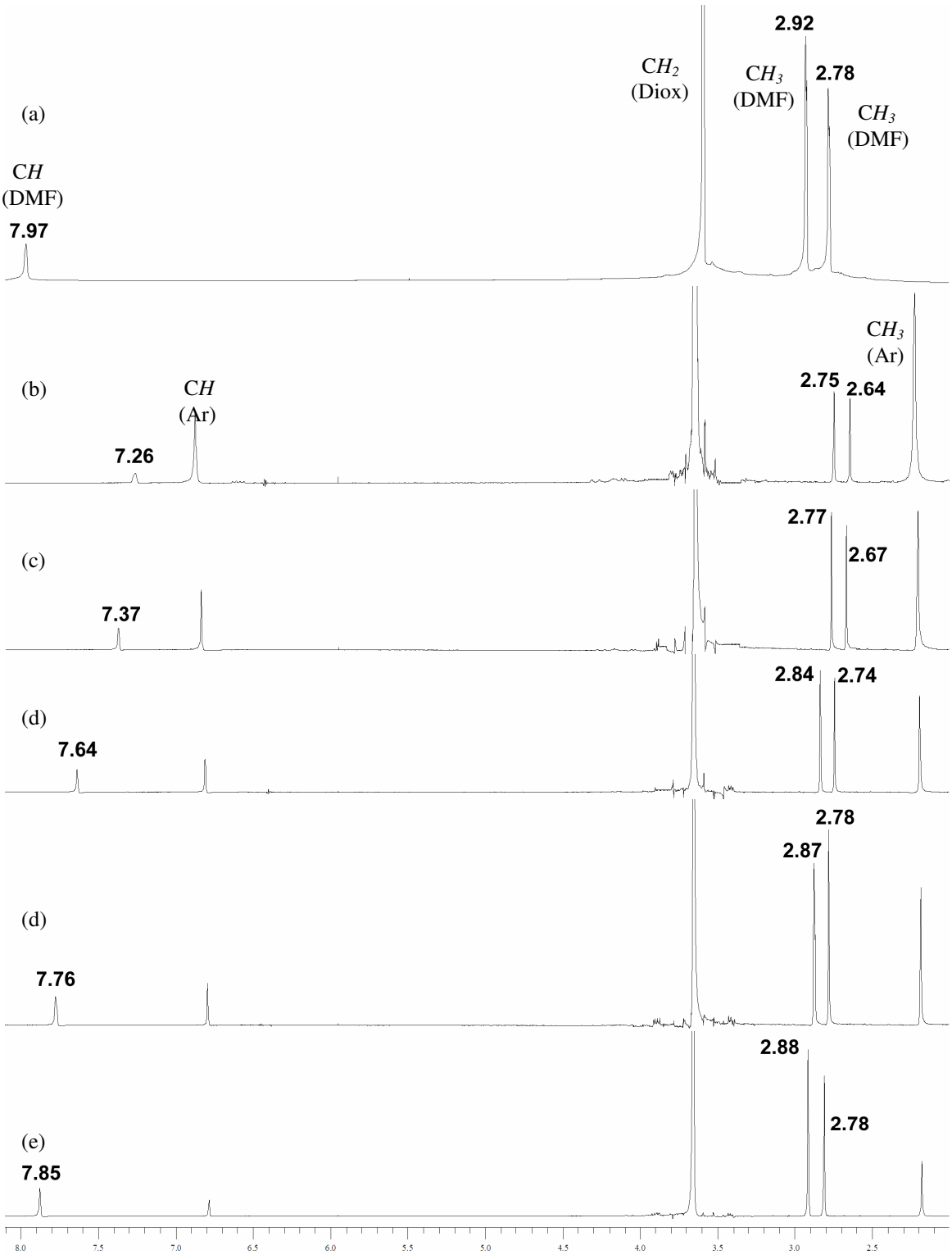

Figure 3.4 ^{1}H NMR titration with (a) DMF in dioxane solvent with a d_{12}-cyclohexane spike, (b) 0.125 equivalents DMF added to a solution of lithium 4-Cl-2,6-dimethylphenoxide in dioxane with a d_{12}-cyclohexane spike, (c) 0.25 equivalents DMF added, (d) 0.65 equivalents DMF added, (e) 1.3 equivalents DMF added, (f) 2 equivalents DMF added.

DFT calculations further support the assessment that DMF is a stronger Lewis base than dioxane. Calculations at the B3LYP/6-31G* level of theory show the replacement of the four dioxane molecules with DMF on the full dimeric aggregate results in an energy gain of 26 kcal/mol (Figure 3.5).

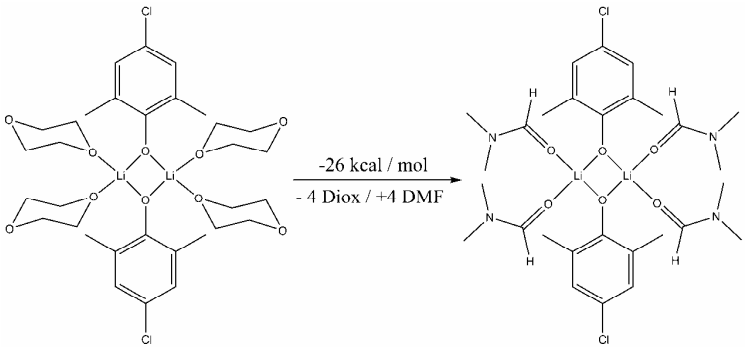

Figure 3.5 Calculation of solvent exchange reaction of the tetrasolvated lithium ring dimer with DMF replacing dioxane. Calculation at B3LYP/6-31G* level of theory.

It is possible that the DMF does indeed bind to the lithium dimer in solution to give the targeted complex $[(4\text{-Cl-2,6-Me}_2\text{-C}_6\text{H}_2\text{OLi})_2\cdot(\text{dioxane})_{1.5}\cdot(\text{DMF})]_\infty$. This may then be used as a precursor building block for the 6^3-net assembly found for **3.2**. However, since the solvent media used for the reaction was dioxane and is present in a large excess, the coordinated DMF is replaced by the dioxane during crystallization. Nevertheless, the goal of altering the topology of the 4^4-net to a 6^3-net has been achieved (Figure 3.3c).

Although our attempt to coordinate one DMF per dimer resulted in the formation of **3.2**, we still proceeded to the next stage in the stepwise site reduction of the dimer, as shown in Scheme 3.1. However, the addition of 2 equivalents of DMF per dimer resulted

in the formation of the dioxane-free DMF solvate $[(4\text{-Cl-2,6-Me}_2\text{-C}_6\text{H}_2\text{OLi})_4\cdot(\text{dmf})_4]$ (**3.3**).

Complex **3.3** forms a tetrameric cubane aggregate where each of the lithium centers are coordinated by a DMF molecule (Figure 3.6). As a further indication of the Lewis base strength of DMF, the Li-O_{DMF} distance of 1.937(3) Å is *shorter* than all of the Li-O_{Ar} distances, which range between 1.978(3) – 2.030(3) with a mean of 2.001 Å. As a comparison, the mean Li-O_{diox} distances in **3.1**-**3.10** are between 0.076 – 0.164 Å longer than the corresponding mean Li-O_{Ar} distances.

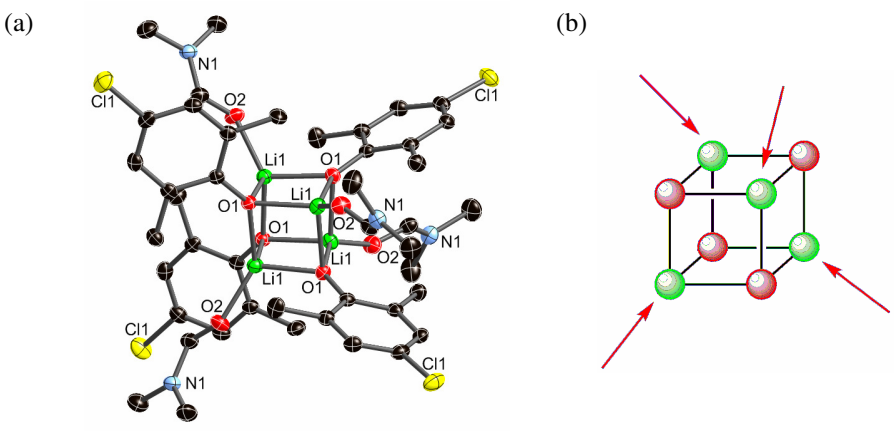

Figure 3.6 (a) The tetrameric cubane aggregate of **3.3** with all four lithium centers solvated by a DMF molecule. Hydrogen atoms are removed for clarity. (b) Illustration of the tetramer with DMF molecules shown as terminal red arrows.

An unanticipated effect of replacing the coordinated dioxane with DMF is the increase in aggregation from a dimer to a tetramer. A common paradigm in *s*-block metal chemistry is that increasing the polarity of the solvent leads to a decrease in aggregation state. This is due to the increased strength of the M-O_{solv} interactions. However, there are some noted cases where the reverse effect is true. For example, Collum reported a series of R_2NLi-LiX mixed aggregates where the solution aggregation state increased upon the

addition of the strong Lewis base hexamethylphosphoramide (HMPA).[7] Also, in a more relevant example, Jackman reported that dimeric lithium phenoxides in THF solutions form tetramers upon the addition of the strong Lewis base HMPA.[8]

The addition of more equivalents of DMF per lithium, *i.e.* 4 eq. per dimer, again resulted in the formation of the molecular DMF solvate **3.3**. Therefore, out of the four targeted DMF site reduction complexes shown in Scheme 3.1 only two formed, with both having unexpected modifications. The targeted 6^3-net, **3.2**, was synthesized from trigonal nodes as desired, but the nodes were made with a terminal dioxane instead of a terminal DMF. The molecular DMF solvate was also synthesized, but our targeted complex was a dimeric aggregate where each metal was disolvated. The complex synthesized however, **3.3**, is a tetrameric cubane where all the metals are monosolvated.

At this stage, we decided to modify our synthetic approach by changing solvent conditions. In the reactions discussed thus far, dioxane was used as the bulk solvent. We decided to use toluene, which is a less polar solvent, to encourage the formation of the larger tetrameric aggregates. This system would now also allow the use of substoichiometric equivalents of both dioxane and DMF to control the points of network extension from each tetrameric node. As shown in Scheme 3.2, our expectation was that the following reduction in network structure would occur: (i) a 2D 6^3-net, (ii) a 1D polymer, (iii) a 0D dumbbell, and (iv) a molecular DMF solvate.

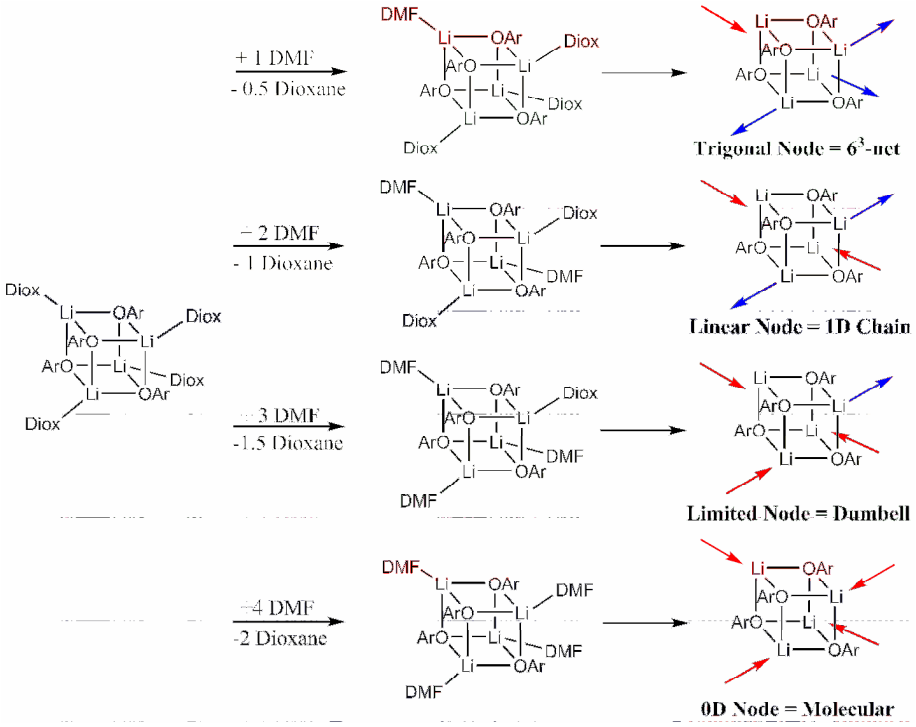

Scheme 3.2 Proposed sequential replacement of dioxane by DMF starting with a dioxane solvated tetramer. The amount of each Lewis base is relative to the tetramer. The dioxane is half the amount of DMF in each step because it is a divergent solvate that bridges between aggregates.

The first part of the project was to target the dioxane solvated tetramer using a less polar solvent. We were encouraged that tetrameric aggregate may be energetically favorable in this system because of the formation of the DMF tetramer **3.2**. Indeed, a tetrameric dioxane solvate, $[(4\text{-Cl-}2,6\text{-Me}_2\text{-C}_6\text{H}_2\text{OLi})_4\cdot(\text{dioxane})_2]_\infty$ (**3.5**), is synthesized upon optimizing reaction conditions. The structure of **3.5** is composed of a tetrameric aggregate where three of lithium centers are coordinated by dioxane molecules but the fourth lithium is completely unsolvated (Figure 3.7). Interestingly, only two of the dioxane molecules are divergent to give a one-dimensional coordination polymer.

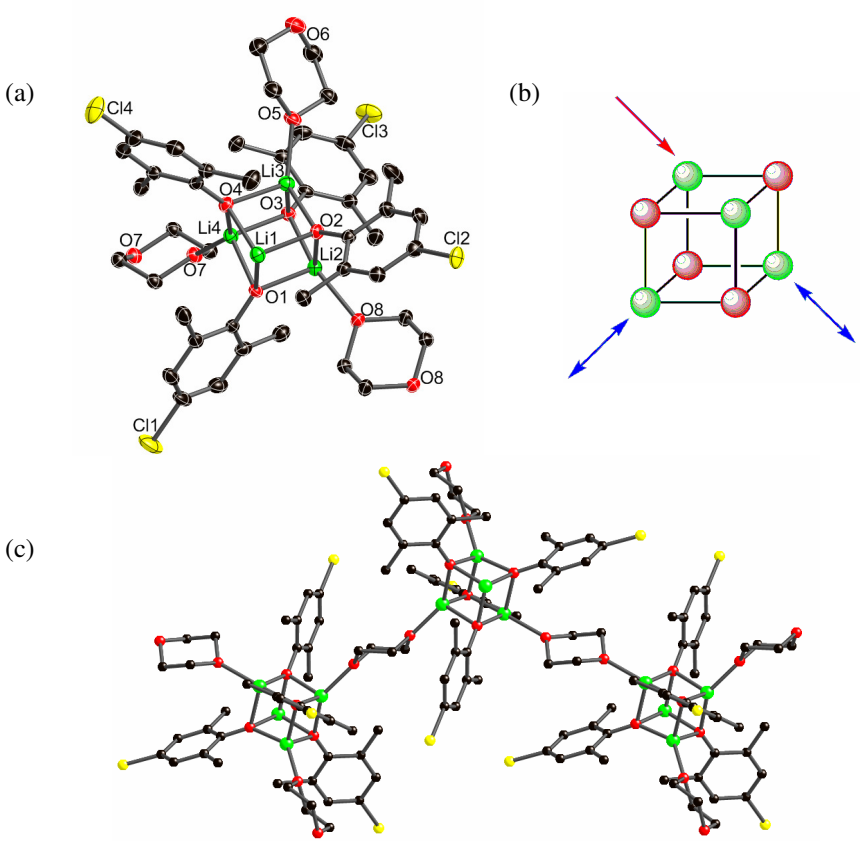

Figure 3.7 (a) Tetrameric aggregate of **3.5** with two of the lithium centers solvated by bridging dioxane, one lithium solvated by a terminal dioxane, and the fourth lithium completely unsolvated. (b) Illustration of the aggregate showing the two bridging dioxanes as blue arrows and the terminal dioxane shown as a red arrow. (c) Extended structure of **3.5** with a 1D zigzag chain topology. Hydrogen atoms removed for clarity.

The most impressive aspect of this system is that three different 'dioxane-only' solvates of lithium 4-Cl-2,6-dimethylphenoxide, **3.1**, **3.2**, and **3.5**, may be prepared using different solvent conditions. This differs from all of the previous lithium and sodium aryloxide systems our group has studied,[1] where only single products were formed. However, none were studied as intensely as this system. Part of the flexibility in this case is that the phenoxide ligand allows the formation of energetically stable dimers, in **3.1** and **3.2** (where the metals are disolvated), and tetramers in **3.5** (where the metals are either monosolvated or unsolvated).

Upon synthesizing the targeted dioxane solvated tetramer, we sought to replace the dioxane in a stepwise manner with terminal DMF as shown in Scheme 3.2. Since there are only three coordinated dioxane molecules on each tetramer, the first complex we attempted to synthesize was the one-dimensional chain by the addition of 2 eq. of DMF and 1 eq. of dioxane per tetramer. However, the complex that crystallized from the toluene solution was the previously characterized DMF solvate, **3.3**. Next, we modified the reaction conditions slightly by using a mixed toluene/hexane solution. Surprisingly, this co-crystallized as two products: (i) the DMF solvate **3.3**, and (ii) the targeted mixed solvent tetramer $[(4\text{-Cl-}2,6\text{-Me}_2\text{-C}_6\text{H}_2\text{OLi})_4\cdot(\text{dioxane})\cdot(\text{dmf})_2]_\infty$ (**3.4**). Crystals of the two complexes have visually distinct morphologies with **3.3** crystallizing as square plates and **3.4** as parallelepipeds.

The mixed solvent complex, **3.4**, forms the desired tetrameric cubane aggregate with two of the lithium atoms coordinated by terminal DMF molecules and the second two lithiums coordinated by bridging dioxane molecules. As in the previous complexes, the M-O_{DMF} of 1.922(2) Å is short compared with the M-O_{Ar} distances of 1.922(2) – 2.049(2) Å (mean of 1.989 Å), whereas the M-O_{diox} distance is 2.125(2) Å. Since there are two divergent dioxane molecules per tetramer, the extended structure forms a one-dimensional chain (Figure 3.8). The addition of more DMF to the system (*i.e.* 3 eq. of DMF per tetramer) gave the DMF solvate, **3.3**, in neat toluene or the mixture of **3.3** and **3.4** in toluene/hexane.

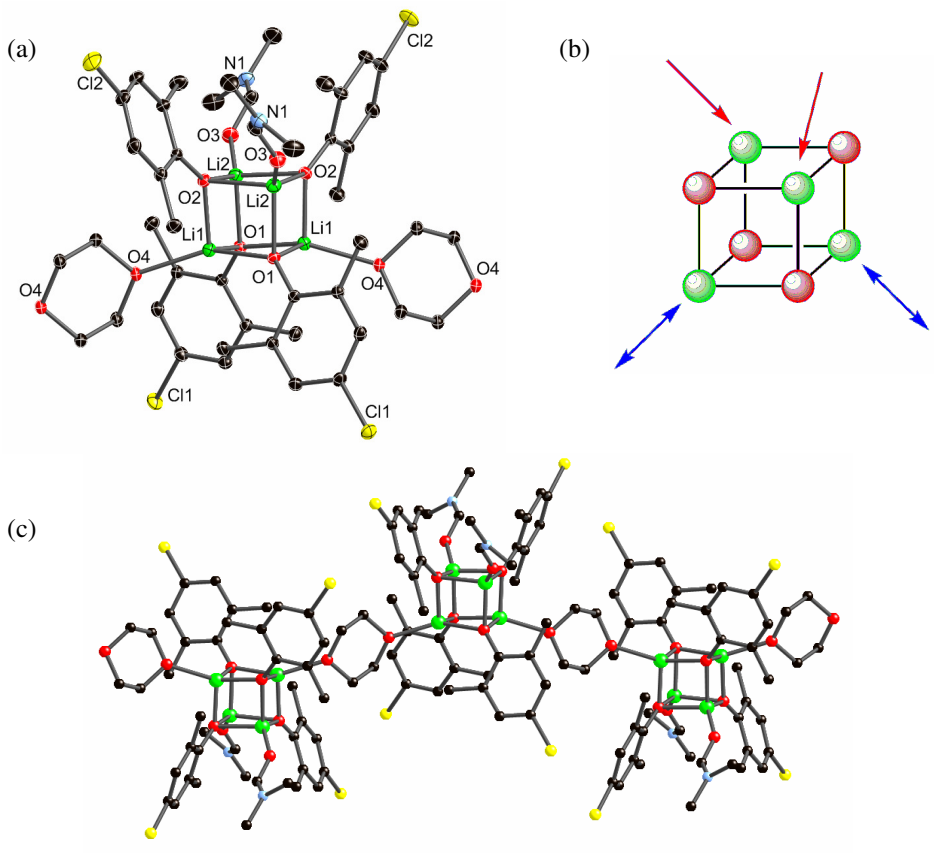

Figure 3.8 (a) Tetrameric aggregate of **3.4** with two of the lithium centers solvated by dioxane and the other two lithium centers solvated by DMF. (b) Illustration of the tetrameric aggregate with bridging dioxane shown as blue arrows and terminal DMF shown as red arrows. (c) The extended 1D zigzag chain of **3.4**.

Since both **3.4** and **3.5** form 1D polymers from tetrameric aggregates, a useful comparison can be made between the metrical parameters of the extended structures. The distance between the Li_4O_4 centroids in **3.4** is 10.089 Å, with this distance in **3.5** similar at 9.916 Å. The 1D chain in **3.4** is substantially more linear than **3.5** with the angle between the centroids being 135.72° in **3.4**, and 117.17° in **3.5**. This comparison is interesting as it illustrates that simply changing the solvation on two of the lithium centers in the cubane results in a large difference in the linearity of the extended structure.

As the last part of our study on lithium 4-Cl-2,6-dimethylphenoxide in different solvents, we synthesized the 1,3-dioxolane solvate $[(4\text{-Cl-2,6-Me}_2\text{-C}_6\text{H}_2\text{OLi})_2\cdot(\text{dioxolane})_2]_\infty$ (**3.6**). The structure forms a dimeric lithium aggregate that is tetrasolvated by dioxolane (Figure 3.9a). The dioxolane molecules act as linear linkers similar to dioxane. Comparison of the metrical parameters in **3.1** and **3.6** reveals that both the localized and the framework geometries are very similar. For example, the mean Li-O_{Ar} bond lengths are 1.861 and 1.890 Å in **3.1** and **3.6**, respectively. The mean Li-O_{Solv} distances are fairly similar as well, being 2.014 and 2.061 Å in **3.1** and **3.6**. The dioxane is a slightly longer linker than dioxolane leading to greater mean separations between neighboring ring centroids of 8.803 Å and 7.526 Å in **3.1** and **3.6**, respectively. Overall, these values demonstrate that dioxane and dioxolane possess comparable properties as didentate linkers.

Although the metrical parameters are similar, the topologies of the extended networks of **3.1** and **3.6** differ. In **3.1**, the dimeric aggregates act as square planar nodes to give a two-dimensional 4^4-network. In **3.6**, the dioxolane-coordinated dimeric aggregates act as tetrahedral nodes to give a three-dimensional diamondoid network (Figure 3.9c,d). From our previous studies of lithium aryloxides with dioxane, we showed that small changes in the aryloxide ligand can have a pronounced influence over the resulting network topology.[1] The change in topology between **3.1** and **3.6** shows that small changes in the divergent linker can also have a similar influence over the network structure.

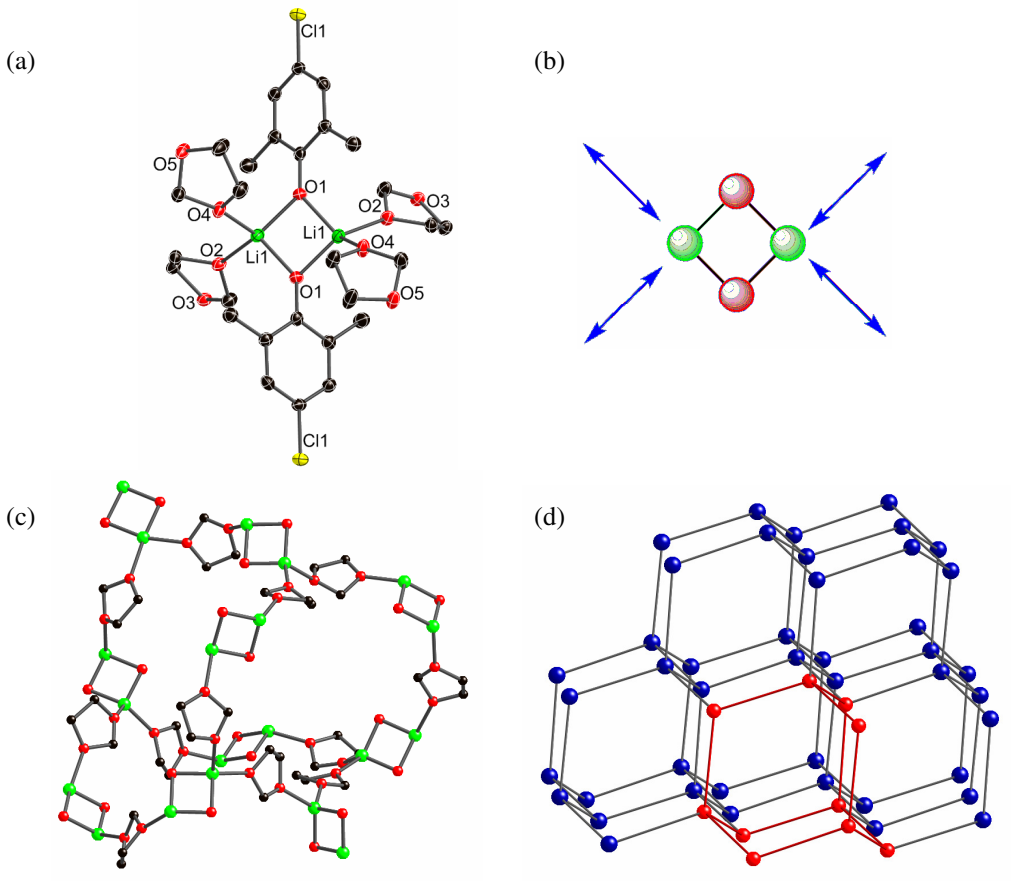

Figure 3.9 (a) The dimeric aggregate of **3.6** with two dioxolane molecules solvating each metal center. (b) Illustration of the dimeric aggregate as a tetrahedral node with the bridging dioxolane shown as blue arrows. (c) Adamantane subunit of the extended structure of **3.6**. Only the Li_2O_2 dimers and bridging dioxolane molecules needed to build the adamantane unit are shown for clarity. (d) The extended structure with diamondoid topology. The dimeric aggregates are shown as blue spheres. The adamantane subunit of the net is highlighted in red.

Rather surprisingly, only a handful of crystal structures containing dioxolane as Lewis base have been reported.[9] Moreover, only two of these complexes, the lithium borohydrides $[LiBH_4{\cdot}(dioxol)]_\infty$ and $[LiB(NMe_2)H_3{\cdot}(dioxol)]_\infty$, form coordination polymers (both adopt 2D nets).[10]

3.3 Reactions of Lithium 4-Br-2,6-Dimethylphenoxide

3.3.1 Synthesis

The equimolar reaction of 4-Br-2,6-dimethylphenol with BuLi in 1,4-dioxane resulted in the instant formation of a precipitate, which dissolved on vigorous heating. High-quality crystals of $[\{(4\text{-Br-2,6-Me-}C_6H_2OLi)_2\cdot(dioxane)_2\}\{(4\text{-Br-2,6-Me-}C_6H_2OLi)_2\cdot(dioxane)_{2.5}\}]_\infty$ (**3.7**) were grown from the reaction solution after optimizing the concentration and temperature for crystal growth. The equimolar reaction of 4-Br-2,6-dimethylphenol with BuLi in 1,4-dioxane with DMF resulted in the formation of both $[(4\text{-Br-2,6-Me}_2\text{-}C_6H_2OLi)_4\cdot(dioxane)_1\cdot(dmf)_2]_\infty$ (**3.8**) and $[(4\text{-Br-2,6-Me}_2\text{-}C_6H_2OLi)_4\cdot(dmf)_4]$ (**3.9**). Finally, the equimolar reaction of 4-Br-2,6-dimethylphenol with BuLi in 1,3-dioxolane resulted in the formation of $[(4\text{-Br-2,6-Me}_2\text{-}C_6H_2OLi)_2\cdot(dioxolane)_2]_\infty$ (**3.10**).

3.3.2 Solid State Structures

As a complement to the lithium 4-Cl-2,6-dimethylphenoxide system, we looked at the closely related 4-Br-2,6-dimethylphenoxide analogue to get a better understanding of the solid-state and solution behavior. The lithiation of the phenol in neat 1,4-dioxane produced crystals of $[\{(4\text{-Br-2,6-Me-}C_6H_2OLi)_2\cdot(dioxane)_2\}\{(4\text{-Br-2,6-Me-}C_6H_2OLi)_2\cdot(dioxane)_{2.5}\}]_\infty$ (**3.7**). The first point of note in **3.7** is the incorporation of the desired tetrasolvated Li_2O_2 dimeric rings as the basic building blocks of the structure. However, unexpectedly there are two distinct types of dimeric SBUs present (Figure 3.10a,b). One set of dimers is four-connected, with all four dioxanes bridging between neighboring aggregates, whereas the second set are three-connected, with only three

bridging dioxanes and a single terminal dioxane. Hence, **3.7** is a binary MOF net composed of an equal distribution of tetrahedral and trigonal nodes. The metrical parameters, listed in Table 3.1, are nearly the same as **3.1** with the difference in the mean Li-O_{Ar} bond distances less than 0.033 Å and the difference in the mean Li-O_{diox} distance less than 0.003 Å.

The extended structure of **3.7** proved to be remarkable. Each trigonal node links to three tetrahedral nodes to form a 2D hexagonal sheet. In turn, the tetrahedral nodes link to three trigonal nodes within the layer but also connect to complementary tetrahedral nodes of a second sheet (Figure 3.10c,d). Overall, this results in the assembly of a unique bilayer structure. Figure 3.10c highlights the use of dioxane molecules as pillars connecting the two hexagonal sheets. Additionally, the terminal dioxane molecules associated with the trigonal nodes can be clearly seen protruding above and below the bilayer. This topology can be described as an intermediate between the archetypal structures of the elemental allotropes black phosphorous and diamond. The extended structure can be classified as a binodal (3,4)-connected net with $(6^3)(6^6)$ topology using Schläfli nomenclature. The three-connected node is surrounded by three 6-membered rings and the four-connected node is surrounded by six 6-membered rings.[11] Only a small number of (3,4)-connected binary MOFs have been characterized to date. These include derivatives of the 3D nets boracite,[12] twisted boracite,[13] Pt_3O_4[14] and cubic C_3N_4,[15] and also an unusual 2D tiling of pentagons.[16]

Although a handful of MOF bilayers derived from pairs of 4^4-nets have been reported, we are unaware of any $(6^3)(6^6)$ MOF bilayers comparable to **3.7**.[17] The closest structural analogues to **3.7** are hydrogen-bonded bilayers. In particular, frameworks

prepared through the combination of guanidinium cations (acting as trigonal nodes) and organodisulfonate anions (acting as the tetrahedral pillars) have been intensively studied due to their tunable host-guest chemistry.[18]

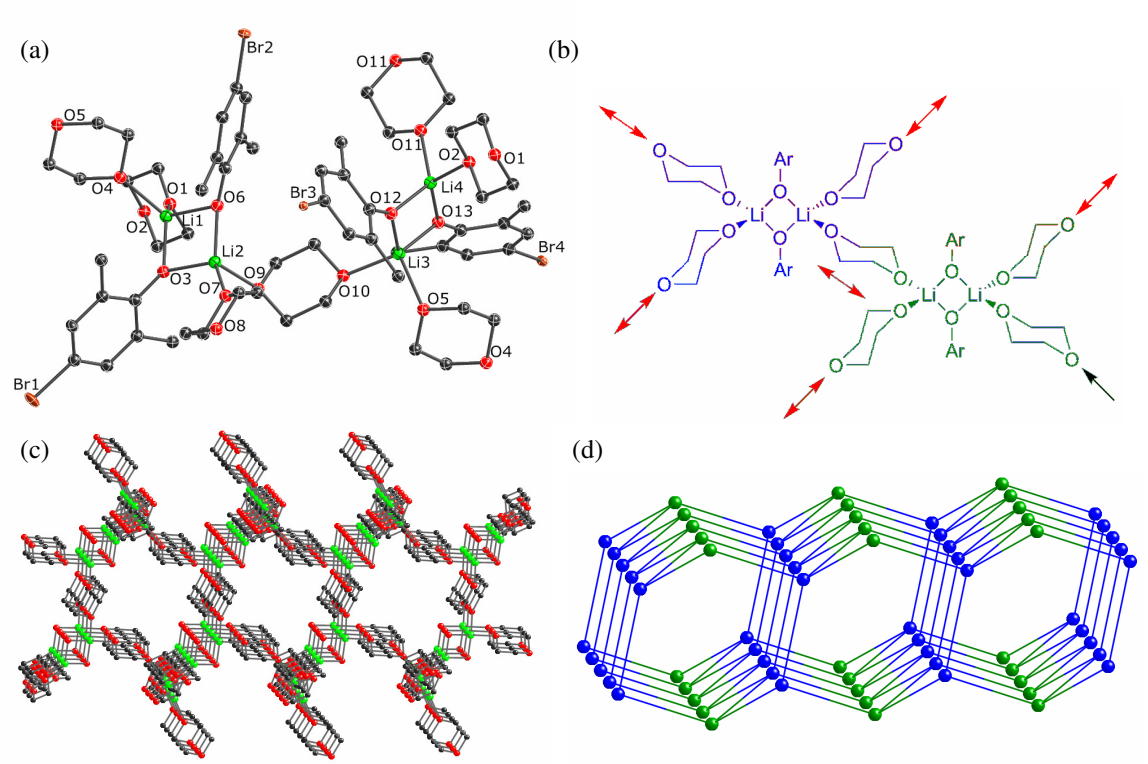

Figure 3.10 (a) The two unique dimeric aggregates within **3.7**, with both dimers tetrasolvated by dioxane. (b) Schematic view of the two types of dimeric SBUs present. The tetrahedral node is shown in blue and the trigonal node is shown is green. The bridging dioxanes are shown as red arrows and the terminal dioxane is shown as a black arrow. (c) Section of the bilayer of **3.7** viewed through the plane of the chair shaped hexagonal nets. Dioxane pillars can be seen bridging between the two layers. Only the oxygen atoms of the aryloxides are shown. Green = lithium, red = oxygen, gray = carbon. (d) A topological representation of **3.7** highlighting the connectivities of the tetrahedral (blue) and trigonal (green) nodes.

An emerging paradigm in MOF crystal engineering is that a relatively small number of high-symmetry topologies dominate.[4] Indeed, two of the most commonly encountered MOF architectures are 2D hexagonal sheets and 3D diamondoid lattices.[19] These are examples of unitary networks constructed by the interconnection of a single

type of node, *i.e.* trigonal or tetrahedral. The structure of **3.7** is an intermediate 'missing link' between these two ubiquitous topologies, a pillared metal-organic bilayer composed of two fused hexagonal nets. This is a rare example of a binary network constructed from both trigonal and tetrahedral nodes, and to our knowledge is an unprecedented topology for a MOF.

Although the parent system, **3.7**, did not give the structure expected, we were still interested in using reaction additives, like DMF, to control the resulting topology of the extended network. However, we were only able to obtain two complexes for this system: $[(4\text{-Br-}2,6\text{-Me}_2\text{-}C_6H_2OLi)_4\cdot(\text{dioxane})_1\cdot(\text{dmf})_2]_\infty$ (**3.8**) and $[(4\text{-Br-}2,6\text{-Me}_2\text{-}C_6H_2OLi)_4\cdot(\text{dmf})_4]$ (**3.9**). Similar to the reaction mixture that produced **3.4**, both of these complexes co-crystallized from a mixed hexane/toluene reaction solution containing 1.5 eq. of dioxane and 1 eq. of DMF per tetramer. The two complexes had visually distinct crystal morphologies, with **3.8** crystallizing as parallelepipeds and **3.9** as square plates.

The structure of **3.8** is similar to **3.4**, forming a tetrameric cubane aggregate with four lithium atoms and four μ_3-aryloxides (Figure 3.11a). Two of the lithium atoms are coordinated by terminal DMF, with the second two lithiums coordinated by bridging dioxane molecules. As was seen in the previous complexes, the $M\text{-}O_{DMF}$ distance of 1.928(2) Å is short in comparison with the $M\text{-}O_{Ar}$ distances, which range between 1.919(2) – 2.062(2) Å (mean of 1.998 Å), whereas the $M\text{-}O_{diox}$ distance is longer at 2.159(2) Å. Since there are two divergent dioxane molecules per tetramer, the extended structure forms a one-dimensional chain (Figure 3.11c). The metrical parameters of the extended structure are very similar to **3.4**. The distance between the Li_4O_4 centroids in **3.4** is 10.089 Å, with the distance in **3.8** very similar at 10.190 Å. The 1D chains in **3.4**

and **3.8** also have nearly the same degree of linearity, with the angle between centroids being 135.72° for **3.4** and 137.06° for **3.8**.

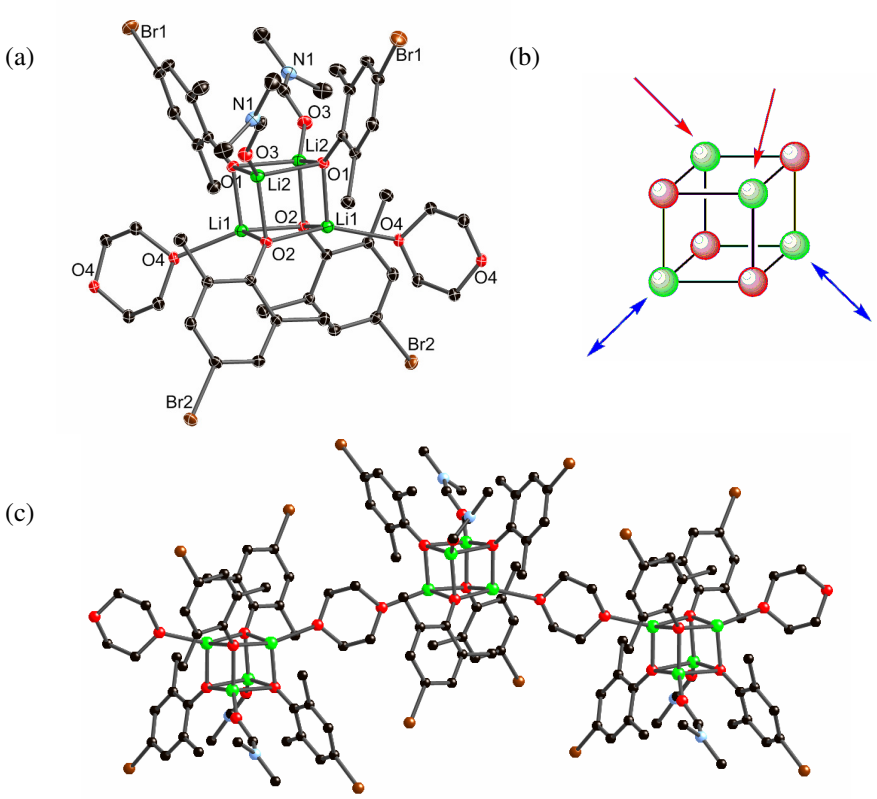

Figure 3.11 (a) Tetrameric aggregate of **3.8** with two of the lithium centers solvated by dioxane and the other two solvated by DMF. (b) Illustration of the tetrameric aggregate with bridging dioxane shown as blue arrows and terminal DMF shown as red arrows. (c) The extended 1D zigzag chain of **3.8**.

The other structure that formed from the same reaction mixture was the DMF solvate $[(4\text{-Br-2,6-Me}_2\text{-C}_6\text{H}_2\text{OLi})_4\cdot(\text{dmf})_4]$ (**3.9**), which is isostructural to the chloro-analogue **3.3**. The structure forms a tetrameric cubane aggregate where each of the lithium centers are coordinated by a DMF molecule (Figure 3.12). The metrical parameters between **3.3** and **3.9** are essentially identical with differences in the mean Li-O_{Ar} and Li-O_{diox} distances being less than 0.004 Å.

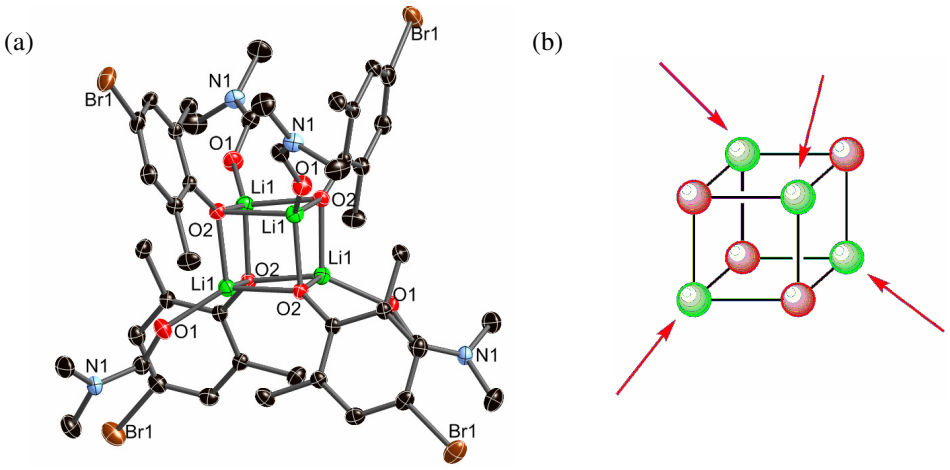

Figure 3.12 (a) Tetrameric cubane aggregate of **3.9** with all lithium centers solvated by DMF. Hydrogen atoms are removed for clarity. (b) Illustration of the tetramer with DMF molecules shown as terminal red arrows.

As a final complementary study to the previous system, we synthesized the dioxolane solvate, $[(4\text{-Br-}2,6\text{-Me}_2\text{-}C_6H_2OLi)_2\cdot(\text{dioxolane})_2]_\infty$ (**3.10**). Structural analysis of complex **3.10** again revealed that the desired tetrasolvated Li_2O_2 ring dimers are retained upon crystallization and act as tetrahedral nodes (Figure 3.13). Overall, this results in the formation of a distorted 3D diamondoid lattice which is isostructural with **3.6**.

Comparison of the metrical parameters between the dioxane and dioxolane solvate, **3.7** and **3.10**, reveals that both the localized and the framework geometries are similar. For example, the mean Li-O_{Ar} bond lengths are 1.894 and 1.898 Å in **3.7** and **3.10**, respectively. Even the mean Li-O_{Solv} distances are fairly close, being 2.017 and 2.070 Å in **3.7** and **3.10**, respectively. As was seen in the previous comparison, dioxane is a slightly longer linker than dioxolane, leading to greater mean separations between neighboring ring centroids, 7.982 Å and 7.589 Å in **3.7** and **3.10** respectively. Finally, the mean angles between these centroids are 109.2° in **3.7** and 108.8° in **3.10**.

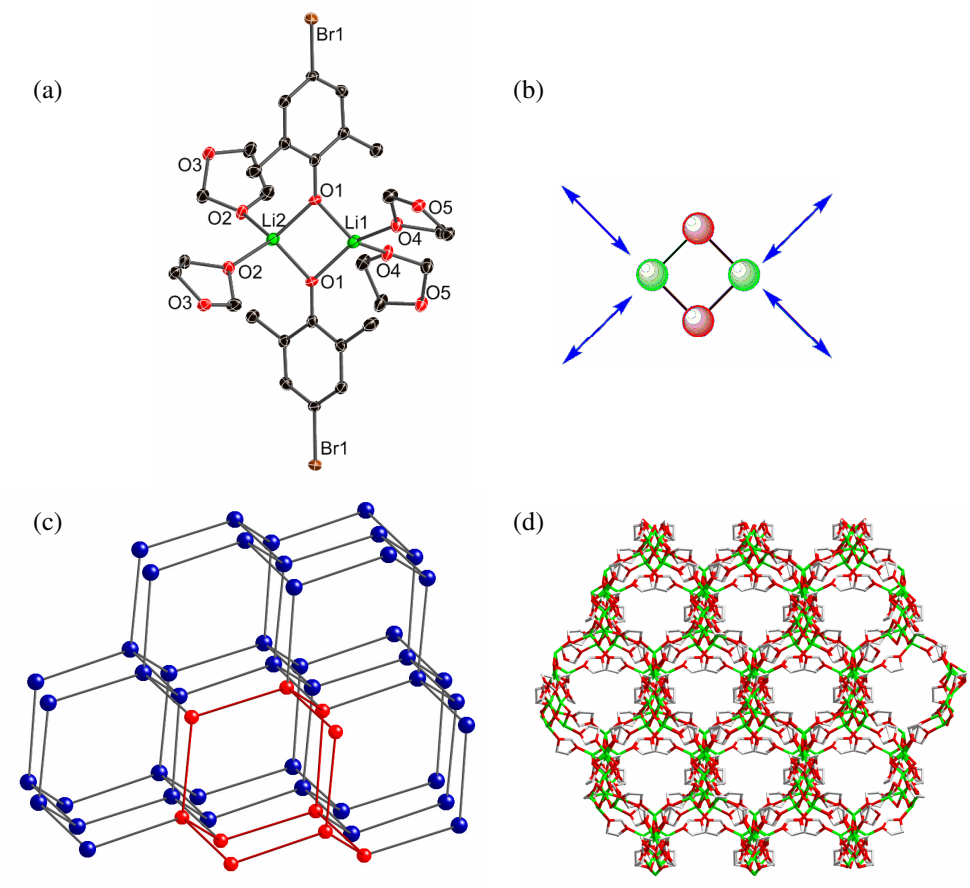

Figure 3.13 (a) Dimeric aggregate of **3.10** with two dioxolane molecules solvating each metal center. (b) Illustration of the dimeric aggregate as a tetrahedral node with the bridging dioxolane shown as blue arrows. (c) Extended structure with a diamondoid topology. The dimeric aggregates are shown as blue spheres. The adamantane subunit of the net is highlighted in red. (d) Section of the extended structure of **3.10** showing a view down the hexagonal *pseudo*-channels. Only oxygen centers of the aryloxides are shown and all hydrogen atoms are removed for clarity. Green=lithium, red=oxygen and grey=carbon.

3.4 Solution Studies

In order to better understand the solid-state aggregates obtained for the lithium aryloxide systems, we conducted a series of solution studies. Studying the solution behavior of *s*-block metal aggregates is generally complicated because of their dynamic behavior. In both of the studies detailed below, the average aggregation state of each

species in solution could be determined, but no information on the degree of solvation is obtained.

3.4.1 Aggregate Size Determination By NMR

Jackman has previously demonstrated that the aggregation state of lithium aryloxides can be correlated with the difference (Δ) between the ^{13}C NMR chemical shift positions of the *para*-carbons of the complex and the corresponding anisole (where Δ values of approximately 4-6, 12-14, and 15-18 ppm correspond with the formation of tetramers, dimers and monomers respectively).[20] The studies looked at a range of phenols in a number of different solvents including pyridine, THF, dimethoxyethane, and dioxolane. The measurements were also taken over several different temperatures to show how temperature affects aggregation. The degree of aggregation was then verified by comparison to other solution methods such as vapor pressure barometry.[21]

We were interested in performing a similar study using both lithium 4-Cl-2,6-dimethylphenoxide and 4-Br-2,6-dimethylphenoxide in dioxane and dioxolane to determine if there is a relationship between the solid-state and solution structures. In order to verify our work, we first studied a number of lithium phenolates in dioxane. All of the reactions had known solid-state structures, forming either dimeric or tetrameric aggregates.

The first step in the study was the preparation of the anisoles for a series of phenols. In the preparation of anisoles reported by Jackman,[20] NaH was used to generate a reactive intermediate. However, we found that replacing NaH with KH leads to improved product purity and yield. The phenols were added to a suspension of KH in Et_2O at 0 ^oC. The resulting mixture was then warmed to room temperature and stirred for

two hours, then quenched with an excess of MeI (4 mL). Stirring was continued for a further 12 h. All volatile organics were removed under vacuum and replaced with water (20 mL). The products were extracted into Et_2O (3 x 20mL), washed with saturated NaOH (30 mL) and dried over $MgSO_4$. The solvent was then evaporated, furnishing the crude methyl ether product as a clear oil, which was then further purified by vacuum distillation. The ^{13}C NMR shift of the anisole in ether dioxane or dioxolane with a deuterated cyclohexane spike was then compared to the corresponding lithium phenolate. The well established shift of the *para*-carbon (δ_{salt} - $\delta_{anisole}$) was used to determine the degree of aggregation.[20] Table 3.2 shows the ^{13}C NMR chemical shifts $\Delta\delta_{(4)}$ (δ - $\delta_{anisole}$) for lithium phenolates in dioxane at 25 ^{o}C.

TABLE 3.2

^{13}C NMR CHEMICAL SHIFT DIFFERENCE $\Delta\delta_{(4)}$ FOR LITHIUM PHENOLATES IN DIOXANE (25 ^{o}C, ~0.5 M) AND CORRESPONDING STRUCTURE

Entry	Aryloxide	$\Delta\delta_{(4)}$, (δ - $\delta_{anisole}$)	Solution	Solid State
I	C_6H_5O-Li	-6.0	Tetramer	Tetramer
II	4- Me-C_6H_4O-Li	-6.8	Tetramer	Tetramer
III	4-MeO-C_6H_4O-Li	-4.4	Tetramer	Tetramer
IV	4-Et-C_6H_4O-Li	-6.3	Tetramer	Tetramer
V	4-*i*Pr-C_6H_4O-Li	-6.3	Tetramer	Tetramer
VI	4-Cl-C_6H_4O-Li	-6.4	Tetramer	Tetramer
VII	4-Br-C_6H_4O-Li	-6.6	Tetramer	Tetramer
VIII	2,4,6-Me_3-C_6H_2O-Li	-12.0	Dimer	Tetramer
IX	2,6-Me_2-C_6H_3O-Li	-18.3	Monomer	Dimer
X	4-Cl-2,6-Me_2-C_6H_2O-Li	-12.5	Dimer	Dimer
XI	4-Br-2,6-Me_2-C_6H_2O-Li	-13.3	Dimer	Dimer

The results in Table 3.2 indicate that there is generally good agreement between the solution aggregates and those found in the solid state for most of the aryloxides. The

only two structures that deviate between solution and the solid-state are 2,4,6-Me-C_6H_2O- and 2,6-Me-C_6H_3O- (Entries **VIII** and **IX**). This may be explained in terms of the steric bulk at both *ortho*- positions, which may lead to little energetic differences between dimeric and tetrameric aggregation in these cases. The results for the solution behavior of **3.1** and **3.7** suggest that the dimeric aggregates seen in the solid-state are also present in solution (Entries **X** and **XI**).

We were further interested in studying the solution behavior of one of the phenols over a range of temperatures. Dioxane could not be used for this study (freezing point = 12 °C), but dioxolane is well suited for this purpose (freezing point = -95 °C). Table 3.3 shows the ^{13}C NMR chemical shifts ($\Delta\delta_{(4)}$ (δ - $\delta_{anisole}$)) for lithium 4-Br-2,6-dimethylphenoxide in dioxolane over the temperature range of -80 ^{o}C to 25 ^{o}C. The results indicate that the room temperature solution studies mirror those at low temperatures. Moreover, the ^{1}H and ^{13}C NMR signals within the dioxolane spectra shift by less than 0.1 and 1 ppm respectively, over the temperature range. This behavior is indicative of a single major solution aggregate being present. Complex **3.7** also gave almost identical Δ values of -13.3 and -13.4 ppm in dioxane and dioxolane solutions (20 ºC, 0.5 M), suggesting similar dimeric aggregation.

TABLE 3.3

^{13}C NMR CHEMICAL SHIFTS $\Delta\delta_{(4)}$ FOR LITHIUM 4-Br-2,6-$Me_2C_6H_2O$- IN DIOXOLANE (~0.5 M)

Phenolate	T(^oC)	$\Delta\delta_{(4)}$	Aggregate
4-Br-2,6-Me_2-C_6H_2O -	25	-13.4	Dimer
	-5	-13.6	Dimer
	-25	-13.8	Dimer
	-60	-14.0	Dimer
	-80	-14.1	Dimer

3.4.2 Aggregate Size Determination By Cryoscopy

A traditional method to study the molecular weight of a compound in solution is through the use of cryoscopy.[22] The molecular weight is determined by comparing the freezing point of a pure solvent with the freezing point on addition of an analyte. The molecular weight can be calculate from Equation 3.1 where the freezing point depression, ΔT, is equal to the mass of the solute, W_s, multiplied by the cryoscopic constant, K_f, divided by the molecule mass, M, and the mass of the solvent, W_b. The cryoscopic constant, K_f, is reliably determined for a solvent by first standardizing the system using a compound of known molecular weight.

$$\Delta T = \frac{1000 \times K_f \times W_s}{W_b \times M} \qquad \textbf{(Eq 3.1)}$$

We were interested in studying the solution behavior of **3.7** by cryoscopy as an extension to the ^{13}C NMR solution work already done on this system in dioxane and dioxolane. In order to study **3.7** by cryoscopy, dioxane was chosen as the solvent, due to the more common cryoscopic solvents benzene and cyclohexane yielding only an insoluble precipitate. Dioxane also has the advantage in this study of having a relatively

high freezing point (12 °C). The disadvantage is that since dioxane readily coordinates to the aggregate, only the degree of aggregation could be reliably. The degree of aggregation, A, is calculated by comparing the theoretical molality, m_t, and the calculated molality, m_c, as defined by Equation 3.2. The theoretical molality is determined by the number of initial moles of unsolvated solute, divided by the mass of dioxane solvent in kilograms, as defined by Equation 3.3. The calculated molality was found by dividing the cryoscopic constant by the freezing point depression, as defined by Equation 3.4.

$$A = \frac{m_t}{m_c} \qquad \textbf{(Eq 3.2)}$$

$$m_t = \frac{\text{Mole}_{\text{solute}}}{\text{Solvent}} \qquad \textbf{(Eq 3.3)}$$

$$m_c = \frac{\Delta T}{K_f} \qquad \textbf{(Eq 3.4)}$$

The cryoscopic determination of the degree of aggregation of lithium 4-Br-2,6-dimethylphenoxide was calculated by Equations 3.2-3.4 over a concentration range of 0.03 – 0.15 M (Table 3.4) with multiple runs at each concentration. The studies in dioxane supported the assignment of dimeric solution aggregation, with a calculated degree of association of 2.13 ± 0.09.

Table 3.4

DEGREE OF AGGREGATION FOR LITHIUM 4-Br-2,6-DIMETHYLPHENOXIDE IN DIOXANE

Concentration (mol/L)	ΔT_f	Degree of Aggregation
0.03	0.079 ± 0.001	2.06 ± 0.04
0.07	0.141 ± 0.004	2.21 ± 0.06
0.11	0.324 ± 0.012	1.98 ± 0.03
0.15	0.322 ± 0.004	2.09 ± 0.04

3.5 Summary

The work presented demonstrates that tetrasolvated Li_2O_2 dimers can be used as SBUs to construct coordination networks. Indeed, the solution studies of both **3.1** and **3.7** show that the dimeric aggregates are retained in solution. The assembly of the 4^4-net in **3.1** and the diamondoid networks in **3.6** and **3.10** was in accord with our initial predictions that the dimeric aggregate can be used as either a square planar or tetrahedral SBUs. The unprecedented bilayer seen in **3.7** is essentially an interrupted diamondoid lattice, and the formation of this new MOF topology illustrates that the use of *s*-block SBUs offer new possibilities in the area of network assembly. No examples of Li_2X_2 trigonal or tetrahedral nodes similar to those present within **3.2, 3.6, 3.7,** and **3.10** have previously been reported, where X = any atom. Moreover, complexes **3.6** and **3.10** are the first reported examples of 3D networks of any type constructed from Li_2X_2 dimers.

By adding reaction additives, like DMF, to the reaction mixtures of both systems, we were able to alter the topology of the resulting network. Much like the work in the previous chapter, there were unexpected changes to the system, such as the increase in the aggregation state from dimeric to tetrameric. However, we were able to take a square

planar node (**3.1**) and by adding varying amounts of DMF reduce the aggregate to a trigonal node (**3.2**), a linear node (**3.4** and **3.5**), and a zero-dimensional node (**3.3**). Finally, by changing the ditopic linker from dioxane to dioxolane we were to able to change the square planar node into a tetrahedral node (**3.6**) to give a three-dimensional network.

3.6 Experimental Section

3.6.1 General Procedures

All experimental manipulations were performed under a dry nitrogen atmosphere using standard Schlenk techniques, or in an argon-filled glovebox.[23] All glassware was flame-dried under vacuum before use. Hexane was dried immediately before use by passage through columns of copper-based catalyst and alumina (Innovative Technology), and stored over 4 Å molecular sieves. Dioxane was purchased from Acros and was distilled over sodium benzophenone under N_2 prior to use. The phenols were purchased from Aldrich and were recrystallized from hexane. BuLi was purchased from Aldrich as a 1.6 M solution in hexane and was standardized by titration against salicylaldehyde phenylhydrazone directly before use. Deuterated solvents were purchased from Cambridge Isotope Laboratories and were dried by storage over 4 Å molecular sieves. ^{1}H and ^{13}C NMR spectra were recorded on a Bruker AVANCE DPX-400 spectrometer at 293 K, and were referenced internally to the residual signals of the deuterated solvents.

3.6.2 X-ray Crystallography

Crystals were examined under Infineum V8512 oil. The datum crystal was affixed to a thin glass fibre mounted atop a tapered copper mounting-pin and transferred to the 100 K nitrogen stream of a Bruker APEX II diffractometer equipped with an Oxford Cryosystems 700 series low-temperature apparatus. Cell parameters were determined using reflections harvested from three sets of 20 0.3° ω scans. The orientation matrix derived from this was passed to COSMO to determine the optimum data collection strategy.[24] Cell parameters were refined using reflections with $I \geq 10\sigma(I)$ harvested from the entire data collection. All data were corrected for Lorentz and polarization effects, as well as for absorption. Tables A.2, A.3, and A.4 list the key crystallographic parameters for **3.1**-**3.10**. The structures were solved and refined using SHELXTL.[25] Structure solution was by direct methods. Non-hydrogen atoms not present in the direct methods solution were located by successive cycles of full-matrix least-squares refinement on F^2. All non-hydrogen atoms were refined with parameters for anisotropic thermal motion. Hydrogen atoms were placed at idealized geometries and allowed to ride on the position of the parent atom. Hydrogen thermal parameters were set to 1.2× the equivalent isotropic U of the parent atom, 1.5× for methyl hydrogens.

3.6.3 Cryoscopy Set-up

The specially designed cryoscopic apparatus (shown in Figure 3.14) is composed of a flat-bottomed inner glass sample tube surrounded by an outer jacket that is vacuum sealed. A fitted side arm with a tap allowed a nitrogen atmosphere to be maintained during measurements. The freezing point were determined by a digital thermometer (Control Company Cat. No. 4000 Traceable® Digital Thermometer, resolution: 0.0001^{o},

accuracy: ± 0.05 ^{o}C) and recorded digitally at 1 second intervals (Control Company Data Acquisition System). The solutions were stirred using a magnetic vortex stirring bar in order to reduce the degree of supercooling. All of the solutions were cooled using an ice bath.

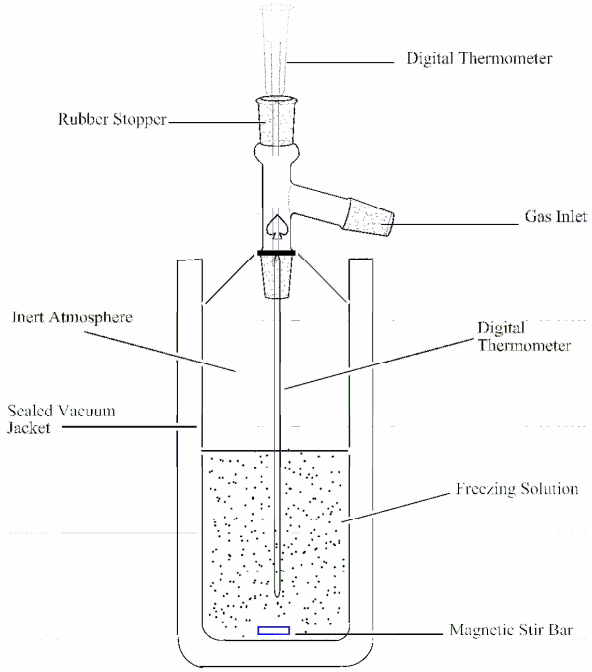

Figure 3.14 General set-up of cryoscopy apparatus

3.6.4 Preparation and Characterization

3.1 [(4-Cl-2,6-Me$_2$-C$_6$H$_2$OLi)$_2$·(dioxane)$_2$]$_\infty$ - BuLi (5 mmol, 3.2 mL) was added to a stirred solution of 4-Cl-2,6-dimethylphenol (5 mmol, 780 mg) in dioxane (7 mL). A white precipitate formed, which completely dissolved on heating the solution to reflux. X-ray quality crystals were obtained by slowly cooling the resulting solution in a hot water bath. Crystalline yield: 730 mg, 57.6 %. δ_H (d_6-DMSO, 293K) 1.95 (s, 12H, *o*-Me), 3.57 (s, 16H, CH_2, dioxane), 6.57 (s, 4H, *o*-H). δ_c (d_{12}-Cyclohexane, 293K) 17.30 (*o*-

Me), 66.66 (CH_2, dioxane), 115.44 (*p*-C, Ph), 125.82 (*o*-C, Ph), 127.23 (*m*-C, Ph), 163.20 (*i*-C, Ph).

3.2 [(4-Cl-2,6-Me_2-$C_6H_2OLi)_2$·(dioxane)$_{2.5}$]$_\infty$ - BuLi (5 mmol, 3.2 mL) was added to a stirred solution of 4-Cl-2,6-dimethylphenol (5 mmol, 780 mg) in dioxane (4 mL) and DMF (0.15 mL). A white precipitate formed, which completely dissolved on heating the solution to reflux. X-ray quality crystals were obtained by slowly cooling the resulting solution in a hot water bath. Crystalline yield: 207 mg, 16.3 %. δ_H (d_6-DMSO, 293K) 1.96 (s, 12H, *o*-Me), 3.57 (s, 20H, CH_2, dioxane), 6.57 (s, 4H, *o*-H). δ_c (d_6-DMSO, 293K) 18.18 (*o*-Me), 66.35 (CH_2, dioxane), 125.48 (*o*-C, Ph), 125.94 (*m*-C, Ph).

3.3 [(4-Cl-2,6-Me_2-$C_6H_2OLi)_4$·$(dmf)_4$] - BuLi (5 mmol, 3.2 mL) was added to a stirred solution of 4-Cl-2,6-dimethylphenol (5 mmol, 780 mg) in dioxane (2.5 mL) and DMF (6.45 mmol, 0.5 mL). A white precipitate formed, which completely dissolved on heating the solution to reflux. X-ray quality crystals were obtained by slowly cooling the resulting solution in a hot water bath. ^{1}H NMR shows only 0.5 equivalents of DMF per aryloxide not 1.0 equivalents as in the crystal structure. Crystalline yield: 527 mg, 41.6 %. δ_H (d_6-DMSO, 293K) 1.97 (s, 24 H, *o*-Me), 2.73 (s, 6H, NCH_3, DMF), 2.89 (s, 6H, NCH_3, DMF), 6.59 (s, 8H, *o*-H, Ph), 7.95 (s, 2H, NCH, DMF). δ_c (d_6-DMSO, 293K) 18.10 (*o*-Me, Ph), 30.78 (NCH_3, DMF), 35.79 (NCH_3, DMF), 109.25 (*p*-C, Ph), 125.90 (*o*-C, Ph), 125.98 (*m*-C, Ph), 162.32 (NCH, DMF), 166.28 (*i*-C, Ph).

3.4 [(4-Cl-2,6-Me_2-$C_6H_2OLi)_4$·(dioxane)·$(dmf)_2$]$_\infty$ - BuLi (5 mmol, 3.2 mL) was added to a stirred solution of 4-Cl-2,6-dimethylphenol (5 mmol, 780 mg) in dioxane (1.875 mmol, 0.16 mL), DMF (1.25 mmol, 0.097 mL), toluene (10 mL), and hexane (5 mL). A white precipitate formed, which completely dissolved on heating the solution to

reflux. X-ray quality crystals were obtained by slowly cooling the resulting solution in a hot water bath. Crystalline yield: 1028 mg, 81.1 %. δ_H (d_6-DMSO, 293K) 1.97 (s, 24 H, *o*-Me), 2.73 (s, 6H, NCH_3, DMF), 2.89 (s, 6H, NCH_3, DMF), 3.57 (s, 8H, dioxane), 6.58 (s, 8H, *o*-H, Ph), 7.95 (s, 2H, NCH, DMF). δ_c (d_6-DMSO, 293K) 18.29 (*o*-Me, Ph), 35.31 (NCH_3, DMF), 35.94 (NCH_3, DMF), 66.51 (CH_2, dioxane), 103.93 (*p*-C, Ph), 125.88 (*o*-C, Ph), 126.12 (*m*-C, Ph), 158.32 (NCH, DMF), 162.47 (*i*-C, Ph).

3.5 $[(4\text{-Cl-}2,6\text{-}Me_2\text{-}C_6H_2OLi)_4 \cdot (dioxane)_2]_\infty$ - BuLi (5 mmol, 3.2 mL) was added to a stirred solution of 4-Cl-2,6-dimethylphenol (5 mmol, 780 mg) in dioxane (2 mL) and hexane (10 mL). A white precipitate formed, which completely dissolved on heating the solution to reflux. X-ray quality crystals were obtained by slowly cooling the resulting solution in a hot water bath. Crystalline yield: 496 mg, 39.1 %. δ_H (d_6-DMSO, 293K) 1.96 (s, 24H, *o*-Me), 3.57 (s, 16H, CH_2, dioxane), 6.57 (s, 4H, *o*-H). δ_c (d_6-DMSO, 293K) 18.18 (*o*-Me), 66.35 (CH_2, dioxane), 125.48 (*o*-C, Ph), 125.94 (*m*-C, Ph).

3.6 $[(4\text{-Cl-}2,6\text{-}Me_2\text{-}C_6H_2OLi)_2 \cdot (dioxolane)_2]_\infty$ - BuLi (5 mmol, 3.2 mL) was added to a stirred solution of 4-Cl-2,6-dimethylphenol (5 mmol, 780 mg) in dioxolane (3.25 mL) A white precipitate formed, which completely dissolved on heating the solution to reflux. X-ray quality crystals were obtained by slowly cooling the resulting solution in a hot water bath. Crystalline yield: 103 mg, 8.5 %. δ_H (d_6-DMSO, 293K) 1.96 (s, 12H, *o*-Me), 3.77 (s, 8H, CH_2, dioxolane), 4.78 (s, 4H, CH_2, dioxolane), 6.58 (s, 4H, *o*-H, Ph). δ_c (d_6-DMSO, 293K) 18.14 (*o*-Me), 63.85 (CH_2, dioxolane), 94.10 (CH_2, dioxolane), 125.74 (*o*-C, Ph), 125.97 (*m*-C, Ph).

3.7 [{(4-Br-2,6-Me-$C_6H_2OLi)_2$·(dioxane)$_2$}{(4-Br-2,6-Me-$C_6H_2OLi)_2$·(dioxane)$_{2.5}$}]$_\infty$ - BuLi (5 mmol, 3.2 mL) was added to a stirred solution of 4-Br-2,6-dimethylphenol (5 mmol, 1010 mg) in dioxane (9 mL) A white precipitate formed, which completely dissolved on heating the solution to reflux. X-ray quality crystals were obtained by slowly cooling the resulting solution in a hot water bath. Crystalline yield: 617 mg, 40.2 %. δ_H (d_6-DMSO, 293K) 1.98 (s, 24H, *o*-Me), 3.56 (s, 36H, CH_2, dioxane), 6.70 (s, 8H, *o*-H). δ_c (d_{12}-Benzene, 293K) 18.40 (*o*-Me), 66.46 (CH_2, dioxane), 103.62 (*p*-C, Ph), 127.80 (*o*-C, Ph), 131.15 (*m*-C, Ph), 164.97 (*i*-C, Ph).

3.8 [(4-Br-2,6-Me_2-$C_6H_2OLi)_4$·(dioxane)$_1$·(dmf)$_2$]$_\infty$ and **3.9 [(4-Br-2,6-Me_2-$C_6H_2OLi)_4$·(dmf)$_4$] -** BuLi (5 mmol, 3.2 mL) was added to a stirred solution of 4-Br-2,6-dimethylphenol (5 mmol, 1010 mg) in dioxane (3.75 mmol, 0.32 mL), dimethylformamide (1.25 mmol, 0.l mL), toluene (20 mL) and hexane (5 mL). A white precipitate formed, which completely dissolved on heating the solution to reflux. X-ray quality crystals of both complexes were obtained by slowly cooling the resulting solution in a hot water bath. The two complexes had distinct crystal morphologies: **3.8** crystallized as parallelepipeds and **3.9** crystallized as square plates. Crystalline yield: 521 mg. δ_H (d_6-DMSO, 293K) 1.97 (s, 6 H, *o*-Me), 2.73 (s, 1H, NCH_3, DMF), 2.89 (s, 1H, NCH_3, DMF), 3.57 (s, 1H, dioxane), 6.70 (s, 2H, *o*-H, Ph), 7.95 (s, 1H, NCH, DMF). δ_c (d_6-DMSO, 293K) 18.05 (*o*-Me, Ph), 30.80 (NCH_3, DMF), 35.81 (NCH_3, DMF), 66.38 (CH_2, dioxane), 96.73 (*p*-C, Ph), 126.88 (*o*-C, Ph), 128.76 (*m*-C, Ph), 162.36 (NCH, DMF), 166.70 (*i*-C, Ph).

3.10 [(4-Br-2,6-Me_2-$C_6H_2OLi)_2$·(dioxolane)$_2$]$_\infty$ - BuLi (5 mmol, 3.2 mL) was added to a stirred solution of 4-Br-2,6-dimethylphenol (5 mmol, 1010 mg) in toluene (20

mL) and dioxolane (9 mL). A white precipitate formed, which completely dissolved on heating the solution to reflux. X-ray quality crystals were obtained by slowly cooling the resulting solution in a hot water bath. The product was found to lose solvent on isolation to give a dioxolane:aryloxide ratio of 0.39:1, as determined by ^{1}H NMR spectroscopy. Crystalline yield: 620 mg, 25.62%. δ_H (d_6-DMSO, 293K) 1.96 (s, 12H, *o*-Me), 3.77 (s, 8H, CH_2, dioxolane), 4.78 (s, 4H, CH_2, dioxolane), 6.58 (s, 4H, *o*-H, Ph). δ_c (d_6-Benzene, 293K) 17.90 (*o*-Me), 65.15 (CH_2, dioxolane), 95.81 (CH_2, dioxolane), 103.44 (*p*-C, Ph), 127.95 (*o*-C, Ph), 130.99 (*m*-C, Ph), 165.01 (*i*-C, Ph).

3.7 References

[1] (a) MacDougall, D. J.; Morris, J. J.; Noll, B. C.; Henderson, K. W. *Chem. Commun.* **2005**, 456. (b) MacDougall, D. J.; Noll, B. C.; Henderson, K. W. *Inorg. Chem.* **2005**, *44*, 1181. (c) Morris, J. J.; Noll, B. C.; Henderson, K. W. *Cryst. Growth Des.* **2006**, *6*, 1071. (d) Morris, J. J.; Noll, B. C.; Honeyman, G. G.; Kennedy, A. R.; Mulvey, R. E.; Henderson, K. W. *Chem. –Eur. J.* **2007**, *13*, 4418. (e) Morris, J. J.; Noll, B. C.; Henderson, K. W. *Chem. Commun.* **2007**, 5191. (f) Morris, J. J.; Noll, B. C.; Schultz, A. J.; Piccoli, P. M. B.; Henderson, K. W. *Inorg. Chem.* **2007**, *46*, 10473.

[2] (a) MacDougall, D. J.; Noll, B. C.; Kennedy, A. R.; Henderson, K. W. *Dalton Trans.* **2006**, 1875. (b) Boyle, T. J.; Pedrotty, D. M.; Alam, T. M.; Vick, S. C.; Rodriguez, M. A. *Inorg. Chem.* **2000**, *39*, 5133.

[3] (a) Rowsell, J. L.; Yaghi, O. M. *Angew. Chem. Int. Ed.* **2005**, *44*, 4670. (b) Dinca, M.; Long, J. R. *J. Am. Chem. Soc.* **2005**, *127*, 9376.

[4] Ockwig, N. W.; Delgado-Friedrichs, O.; O'Keeffe, M.; Yaghi, O. M. *Acc. Chem. Res.* **2005**, *38*, 176.

[5] (a) Bezombes, J. P.; Hitchcock, P. B.; Lappert, M. F.; Merle, P. G. *J. Chem. Soc., Dalton Trans.* **2001**, 816. (b) Clegg, W.; Horsburgh, L.; Couper, S. A; Mulvey, R. E. *Acta Crystallogr., Sect.C* **1999**, *55*, 867. (c) Henderson, K. W.; Dorigo, A. E.; Liu, Q. Y.; Williard, P. G *J. Am. Chem. Soc.* **1997**, *119*, 11855. (d) Durkin, J.; Hibbs, D. E.; Hitchcock, P. B.; Hursthouse, M. B.; Jones, C.; Jones, J.; Malik, K. M. A.; Nixon, J. F. Parry, G. *J. Chem. Soc., Dalton Trans.* **1996**, 3277. (e) Andrews, P. C.; Armstrong,

D. R.; Baker, D. R.; Mulvey, R. E.; Clegg, W.; Horsburgh, L.; O'Neil, P. A.; Reed, D. *Organometallics* **1995**, *14*, 427. (f) Bernstein, M. P.; Romesberg, F. E.; Fuller, D. J.; Harrison, A. T.; Collum, D. B.; Liu, Q. Y.; Williard, P. G. *J. Am. Chem. Soc.* **1992**, *114*, 5100. (g) Bauer, W.; Klusener, P. A. A.; Harder, S.; Kanters, J. A.; Duisenberg, A. J. M.; Brandsma, L.; Schleyer, P. v. R. *Organometallics* **1988**, *7*, 552.

[6] (a) Henderson, K. W.; Kennedy, A. R.; McKeown, A. E.; Strachan, D. *J. Chem. Soc., Dalton Trans.* **2000**, 4348. (b) Karpova, E. V.; Boltalin, A. I.; Korenev, Y. M.; Kemnits, E.; Troyanov, S. I. *Koord. Khim.* **1999**, *25*, 106. (c) Mamak, M.; Zavalij, P. Y.; Whittingham, M. S. *Acta Crystallogr., Sect.C* **1998**, *54*, 937. (d) Markley, T. J.; Toby, B. H.; Pearlstein, R. M.; Ramprasad, D. *Inorg. Chem.* **1997**, *36*, 3376. (e) Lambert, C.; Schleyer, P. v. R.; Pieper, U.; Stalke, D. *Angew. Chem., Int. Ed.* **1992**, *31*, 77.

[7] Romesberg, F. E.; Collum, D. B. *J. Am. Chem. Soc.* **1994**, *116*, 9198.

[8] Jackman, L. M.; Chen, X. *J. Am. Chem. Soc.* **1992**, *114*, 403.

[9] Three complexes containing monodentate 1,3-dioxolane have been characterized: (a) Fromm, K. M.; Gueneau, E. D.; Rivera, J. P.; Bernardinelli, G.; Goesmann, H. *Z. Anorg. Allg. Chem.* **2002**, *628*, 171. (b) Mirsaidov, U.; Shaimuradov, I. B.; Khikmatov, M. *Russ. J. Inorg. Chem.* **1986**, *31*, 1321. (c) Zavalij, P. Y.; Yang, S.; Whittingham, M. S. *Acta Crystallogr., Sect. B* **2004**, *60*, 716.

[10] (a) Giese, H. H.; Nöth, H.; Schwenk, H.; Thomas, S. *Eur. J. Inorg. Chem.* **1998**, 941. (b) Nöth, H.; Thomas, S.; Schmidt, M. *Chen. Ber.* **1996**, *129*, 451.

[11] For a review on network nomenclature see: Delgado-Friedrichs, O.; O'Keeffe, M. *J. Solid State Chem.* **2005**, *178*, 2480.

[12] Abrahams, B. F.; Batten, S. R.; Hamit, H.; Hoskins, B. F.; Robson, R. *Angew. Chem. Int. Ed. Engl.* **1996**, *35*, 1690.

[13] (a) Lu, J.; Mondal, A.; Moulton, B.; Zaworotko, M. J. *Angew. Chem. Int. Ed.* **2001**, *40*, 2113. (b) Chui, S. S. Y.; Lo, S. M. F.; Charmant, J. P. H.; Orpen, A. G. Williams, I. D. *Science* **1999**, *283*, 1148.

[14] Chen, B.; Eddaoudi, M.; Hyde, S. T.; O'Keefe, M.; Yaghi, O. M. *Science* **2001**, *291*, 1021.

[15] Dybtsev, D. N.; Chun, H.; Kim, K. *Chem. Commun.* **2004**, 1594.

[16] Moulton, B.; Lu, J. J.; Zaworotko, M. J. *J. Am. Chem. Soc.* **2001**, *123*, 9224.

[17] For a recent review of network topologies see: Hill, R. J.; Long, D. L.; Champness, N. R.; Hubberstey, P.; Schröder, M. *Acc. Chem. Res.* **2005**, *38*, 337.

[18] Holman, K. T.; Pivovar, A. M.; Swift, J. A.; Ward, M. D. *Acc. Chem. Res.* **2001**, *34*, 107.

[19] James, S. L. *Chem. Soc. Rev.* **2003**, *38*, 176.

[20] (a) Jackman, L. M.; DeBrosse, C.W. *J. Am. Chem. Soc.* **1983**, *105*, 4177. (b) Jackman, L. M.; Smith, B. D. *J. Am. Chem. Soc.* **1988**, *110*, 3829.

[21] Fraenkel, G.; Beckenbaugh, W. E.; Young, P. P. *J. Am. Chem. Soc.* **1976**, *98*, 6878.

[22] Davidson, M. G.; Snaith, R.; Stalke, D.; Wright, D. S. *J. Org. Chem.* **1993**, *58*, 2810.

[23] Schriver, D. F.; Drezdon, M. A. *The Manipulation of Air-Sensitive Compounds*, Wiley, New York, **1986**.

[24] J. Kaercher, *COSMO,* Bruker-Nonius AXS, Inc., Madison, Wisconsin, USA, **2003**.

[25] G. M. Sheldrick, University of Göttingen, Göttingen (Germany), **2001**.